GEM Detectors in Experiments at e$^+$e$^-$ Colliders in BINP

T.V. Maltsev

Budker Institute of Nuclear Physics SB RAS, Novosibirsk, Russia
Novosibirsk State University, Novosibirsk, Russia

Abstract

Micro-pattern gaseous detectors possess a high spatial resolution in the tens of microns, together with a high rate capability of up to 10^7 cm^{-2} s^{-1}. In addition, they have all the advantages of gaseous detectors, such as relatively low cost per unit area and the possibility of equipping a large area, as well as high uniformity. Detectors based on cascaded gas electron multipliers (GEMs) are used in the collider experiments at the Budker Institute of Nuclear Physics (BINP), and are being developed for a number of new projects. In this article, a review of GEM-based detectors for the tagging system of the KEDR experiment at the VEPP-4M collider and for the DEUTERON facility at the VEPP-3 storage ring is presented. The GEM detector application of the CMD-3 detector upgrade at the VEPP-2000 collider and the Super c–τ Factory detector are discussed.

Keywords

KEDR experiment; DEUTERON facility; CMD-3 detector; Super c–τ Factory; gas electron multiplier.

1 Introduction

Cascaded gas electron multipliers (GEMs) [1] provide an opportunity to create large area detectors that are characterized by good spatial resolution and high rate capability [2–6]. Spatial resolution at the range of 50–70 μm can be achieved for relativistic charged particles with triple-GEM cascades operating with argon gas with a CO_2 admixture of 25% [2, 6]. Tracking detectors based on triple-GEM cascades are being developed and used in several experiments at the Budker Institute of Nuclear Physics (BINP).

In this paper, we will review the current status of the triple-GEM detectors for the tagging system (TS) of the KEDR detector [7–9] at the VEPP-4M [10, 11] collider and the light triple-GEM detectors for the photon tagging system (PTS) of the DEUTERON facility [12, 13] at the VEPP-3 storage ring [14]. The KEDR detector is a general-purpose detector installed at the VEPP-4M collider for experiments with electron–positron beams in the energy range 2–10 GeV in the centre-of-mass energy frame. The VEPP-4M is the electron–positron collider at BINP, working in the energy range 1–5 GeV per beam. The DEUTERON facility is a facility with an internal target at the VEPP-3 storage ring, intended for experiments with electrons or positrons, interacting with protons and deuteron nuclei. The VEPP-3 is the injection storage ring for the VEPP-4M collider; it can operate as a storage ring for electrons and positrons up to 2 GeV. Also, the VEPP-3 can operate as a synchrotron radiation source and as a beam source for the DEUTERON facility. We will discuss future GEM applications, including the large cylindrical triple-GEM detector for the cryogenic magnetic detector (CMD-3) at the VEPP-2000 collider and GEMs for a vertex detector of the future Super c–τ Factory [15, 16].

The TS is designed for the detection of electrons and positrons scattered after two-photon interaction. It consists of a magnet system and eight so-called co-ordinate stations—four stations at the electron side and four stations at the positron side. Each co-ordinate station includes a hodoscope of drift tubes and a triple-GEM two-dimensional detector. The TS is described in detail in Ref. [6].

The DEUTERON facility with internal target at the VEPP-3 storage ring [12, 13] is focused on experiments for the study of interactions of electrons, positrons, and photons with light nuclei. A major part

of the experimental programme at DEUTERON is devoted to the measurement of polarized observables in electro- and photo-nuclear reactions. Further progress in these experiments at VEPP-3 is associated with the development of the 'almost-real PTS' [4, 17]. Here, an 'almost-real photon' is a virtual photon with a virtuality $Q^2 = 8$–15 fm^{-2}. The PTS includes a set of magnets and high-resolution tracking detectors that measure the momentum of an electron that has lost a large fraction of its energy via photon radiation, producing a photo-nuclear reaction in the target. The results of spatial resolution measurements of the triple-GEM detector for the DEUTERON facility are presented in this article.

The CMD-3 is installed at the VEPP-2000 collider [15, 18, 19] and is used for measurements of the total cross-section of electron–positron annihilation to hadrons in the operating energy range from 0.32 GeV to 2.00 GeV. The CMD-3 enables the study of light vector mesons as well as n$\bar{\text{n}}$ and p$\bar{\text{p}}$ production cross-sections near the threshold of the reactions in the energy range from 0.32 GeV to 2.00 GeV in the centre-of-mass frame. Among other subsystems, the CMD-3 has a so-called Z-chamber, a thin cylindrical multiwire proportional chamber (MWPC) surrounding the drift chamber. It measures a co-ordinate position along the beam of tracks and provides a signal for the first-level trigger. This chamber is about 20 years old and needs to be replaced. A new GEM-based cylindrical chamber was proposed for this purpose with improved parameters, which include better spatial resolution, trigger segmentation, and rate capability. Together with a new Z-chamber, new endcap GEM-based tracking detectors were proposed. They will be installed between the flanges of the drift chamber and the endcap BGO (Bi$_4$Ge$_3$O$_{12}$) crystal-based calorimeters. These detectors will provide precise track angle determination and trigger signals. The endcap tracker will significantly improve detection efficiency for multihadron events.

The Super c–τ Factory [16] is expected to be built at BINP. The electron–positron collider will operate in the centre-of-mass energy range 2–5 GeV with a peak luminosity of about 10^{35} cm^{-2} s^{-1} and longitudinally polarized electrons. The study of rare decays of D-mesons and τ-lepton decays requires a general-purpose magnetic detector. It is anticipated that the detector will comprise standard subsystems. GEM-based co-ordinate detectors are proposed for the time projection chamber (TPC) because GEMs are considered to provide an acceptable rate capability (10^6 cm^{-2} s^{-1}) as well as spatial resolution in the scale of tens of microns.

2 Triple-GEM detectors for the tagging system of the KEDR experiment at the VEPP-4M collider

The TS of the KEDR detector at the VEPP-4M electron–positron collider [7, 20] is intended for the study of two-photon processes in electron–positron interactions [8]. The TS uses the accelerator magnets as a spectrometer, as shown in Fig. 1. Electrons and positrons leave the interaction point at a very small polar angle after losing a fraction of their energy in photon–photon interactions. These particles pass through an area with a vertical magnetic field and are deflected at a larger angle than the particles of the initial energy (which have not interacted). Thus, electrons and positrons that participated in the photon–photon interaction are taken away from the equilibrium orbit and are detected in one of four TS stations (TS$_1$–TS$_4$). These particles will be referred to as scattered electrons in this paper. Particles of the initial energy remain at the equilibrium orbit. The quadrupoles focus scattered electrons in such a way that their transverse co-ordinates in the detector planes depend weakly on their emission angle. Thus, by measuring the co-ordinates, one can determine the scattered electron energy with a resolution of better than 10^{-3} (r.m.s.) of the beam energy.

The TS includes eight stations based on drift tube hodoscopes combined with high-resolution two-co-ordinate detectors based on triple-GEMs placed in front of each station. The GEM detectors improve the spatial resolution from 300 μm to 65 μm in the orbit plane and provide the possibility of single bremsstrahlung background rejection [6, 21, 22].

Each GEM detector comprises a cascade of three GEMs with a spacing of 1.5 mm. Each GEM has a hexagonal structure of holes of 80 μm in diameter with a pitch of 140 μm. The GEM thickness is
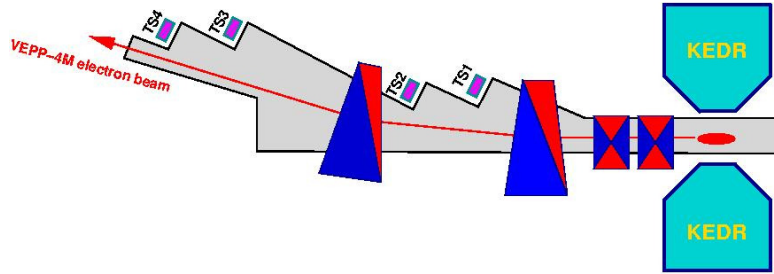
Fig. 1: KEDR tagging system
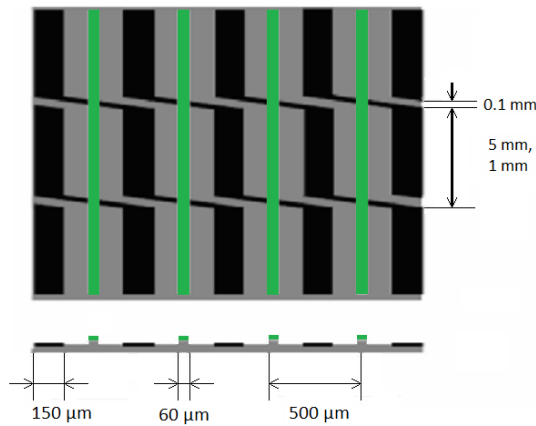
Fig. 2: PCB with small angle stereo readout. Straight strips are marked in green, stereo strips in black. Straight sections of the stereo strips have different lengths, depending on their positions in the detector. This is marked as 1 mm and 5 mm pointing at the straight section.

50 μm. The distance between the bottom GEM and the readout printed circuit board (PCB) is 2 mm and the distance between the top GEM and the drift electrode is 3 mm.

The PCB contains two layers, shown schematically in Fig. 2. The top layer contains straight, 60 μm wide strips. The bottom layer consists of 150 μm wide strips that are divided into straight sections and bridges connecting neighbouring sections so that this strip is, on average, inclined at a certain angle relative to the straight strips. The resulting inclined strips are called stereo strips. Such a configuration of the bottom layer provides uniform charge induction that does not depend on the position along a strip. Straight sections of the stereo strips have different lengths depending on their position in the detector. In the central area, up to 1 cm from the central plane of the detector, the straight sections are 1 mm long; this makes the angle between the stereo and straight strips equal to 30°. Outside this area, the straight sections are 5 mm long and the angle between the stereo and straight strips is close to 11°. Such a layout provides better spatial resolution in the vertical direction in the central area (than outside the central area), which corresponds to the region where electrons and positrons hit the detector. In both layers, the strip pitch is 0.5 mm. The strips in the bottom layer are shifted with respect to the strips in the top layer by 250 μm. The GEMs and PCBs were produced by the CERN PCB workshop.

A detailed discussion of the performance of the TS GEM detectors is presented in Ref. [6], as well as the results from the first long run within the KEDR detector in 2010–2011. During the first run with the KEDR detector, all the TS detectors demonstrated efficiencies between 95% and 98% at a gain between 20 000 and 40 000 [4, 6]. The determined spatial resolution of the detectors for TS KEDR was equal to (65 ± 3) μm for orthogonal electron tracks.

3 Light triple-GEM detectors for the DEUTERON facility at the VEPP-3 storage ring

The DEUTERON facility uses an internal gas target in the VEPP-3 electron storage ring for nuclear physics experiments. This method was proposed and first used in the late 1960s at BINP [12, 13]. The DEUTERON internal gas target [23] consists of polarized deuterium atoms injected in the form of a jet with an intensity of 8×10^{16} atoms/s into a thin-walled T-shaped storage cell with open edges. A series of experiments has been completed during the last decades, all utilizing the tensor-polarized deuterium target to measure tensor asymmetries in fundamental nuclear reactions, such as elastic electron–deuteron scattering and two-body deuteron photo-disintegration.

Further progress of the experiments focusing on the study of photo-nuclear processes can be achieved with the 'almost-real PTS' [13]. The PTS will provide the possibility of performing new measurements of the polarized observables in photo-nuclear reactions with higher photon energies— up to 1.5 GeV—and with higher precision than was achievable before. For example, measurement of tensor target asymmetry and photon beam asymmetry in the deuteron photo-disintegration experiment at large photon energies becomes feasible. Such data are of special interest after the Jefferson Lab has demonstrated that for unpolarized measurements the transition from a meson–nucleon to a quark–gluon description of the reaction has already been observed at an energy of approximately 1 GeV [17].

The PTS is located inside the experimental straight-line section and does not disrupt the storage ring beam optics (Fig. 3). It has three 'warm' dipole magnets (D1, D2, D3) building a chicane, with magnetic field integrals of 0.248 T m, 0.562 T m, and 0.314 T m, respectively. The internal target storage cell is placed between the first and second magnets. The second dipole magnet, together with the tracking system, serves as a magnetic spectrometer for those electrons that lost a fraction of their energy through radiation of an energetic photon producing a photo-reaction on the target. Such electrons are deflected from the beam trajectory by the strong field (1.7 T for a 2 GeV electron beam) of the second magnet, such that they leave through a thin beryllium window from the vacuum chamber of the storage ring. The system of position-sensitive detectors based on cascaded GEMs determines the tracks of these electrons. The trigger sandwich scintillator S2 is located behind the position-sensitive detectors. The main background process for the reaction of a virtual photon exchange reaction is the bremsstrahlung of electrons or positrons on the target nuclei. The veto sandwich scintillator (S1) detects photons from bremsstrahlung processes on the target, which allows most of such background events to be rejected. Three triple-GEM detectors have been planned for installation at the PTS. The first detector for the PTS was mounted with new electronics and tested in the first half of 2013. In general, the detector design is very similar to that of the detectors for the KEDR TS. The detector sensitive area is 160 mm × 40 mm. The readout board contains two layers: the inclined and the straight strips. The inclination angle is 30°. Multiple scattering in the detector material affects the angular resolution in the PTS, unlike the KEDR TS, where only one high-resolution detector is installed just after the outlet window at each station. To minimize multiple scattering due to the detector elements, the thickness of copper on the electrodes at each GEM side was reduced with respect to the regular GEM-based detector layout, to 1–2 μm. Such an approach was investigated previously [24] and it was found that the thinning of copper layers does not affect the detector performance.

The amount of material in the detector was measured, using 100 MeV electrons in the experimental set-up shown in Fig. 4. The angular distribution of the tracks after multiple scattering in the detector under study showed that the amount of material in the detector corresponds to $X/X_0 = (2.4 \pm 0.5) \times 10^{-3}$. This value in turn means that the copper thickness in the GEMs and the PCB is approximately
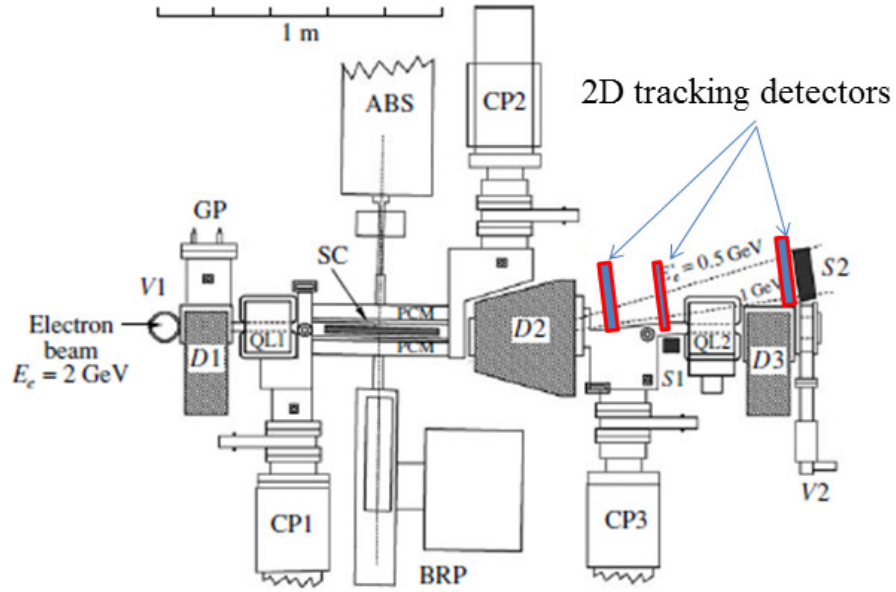
Fig. 3: 'Almost-real photon tagging system' (view from top). D1, D2, D3: three dipole magnets; QL1, QL2: quadrupole lenses; PCM: target polarization control magnet; S1, S2: trigger sandwich scintillators; ABS: polarized atomic beam source; SC: target storage cell; BRP: Breit–Rabi polarimeter for ABS jet atoms; CP1, CP2, CP3, GP: cryogenic and getter pumps; V1, V2: gate valves of the experimental section.
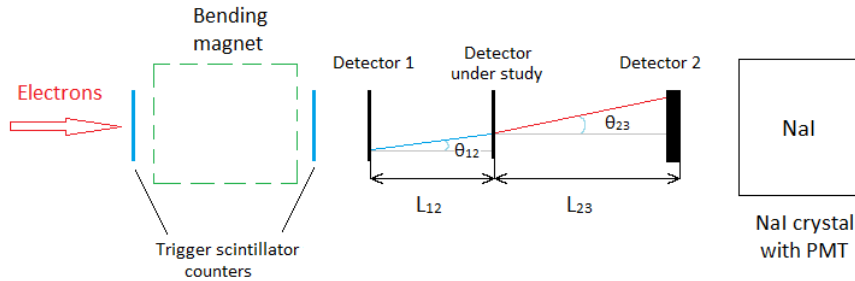

Fig. 4: Set-up for measurement of the material budget and the spatial resolution of the detector

3 µm. The spatial resolution of the detector under study was measured with the same set-up (Fig. 4), but the distances between the detectors were reduced to approximately 75 mm and the beam energy was increased to 1 GeV (Fig. 5) to reduce multiple scattering. The uncertainties in Fig. 5 represent the statistical errors. The curve in Fig. 5 was calculated using the formula of the quadratic sum of the resolution for orthogonal tracks and track projection to the detector plane,

$$\sigma = \sqrt{\sigma_0^2 + (L \times \tan(\alpha))^2/12}, \tag{1}$$

where σ_0 is chosen near the minimum value of the spatial resolution, L is the width of the drift gap, which is equal to 3 mm, and α is a track angle. The effects of multiple scattering and limited spatial resolution
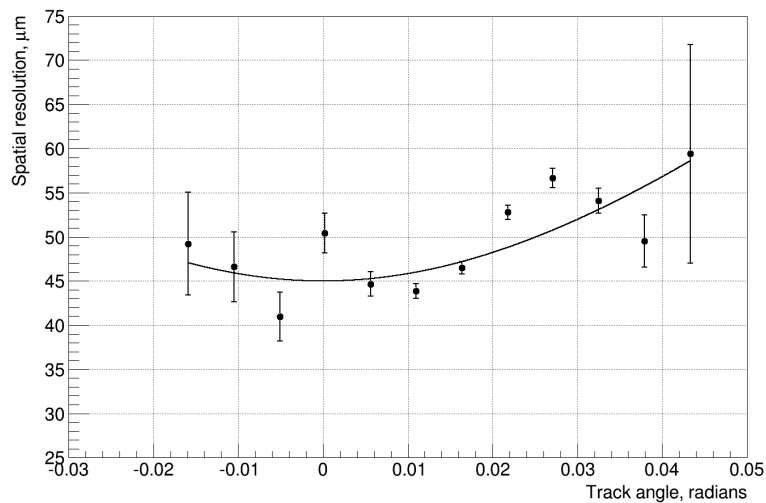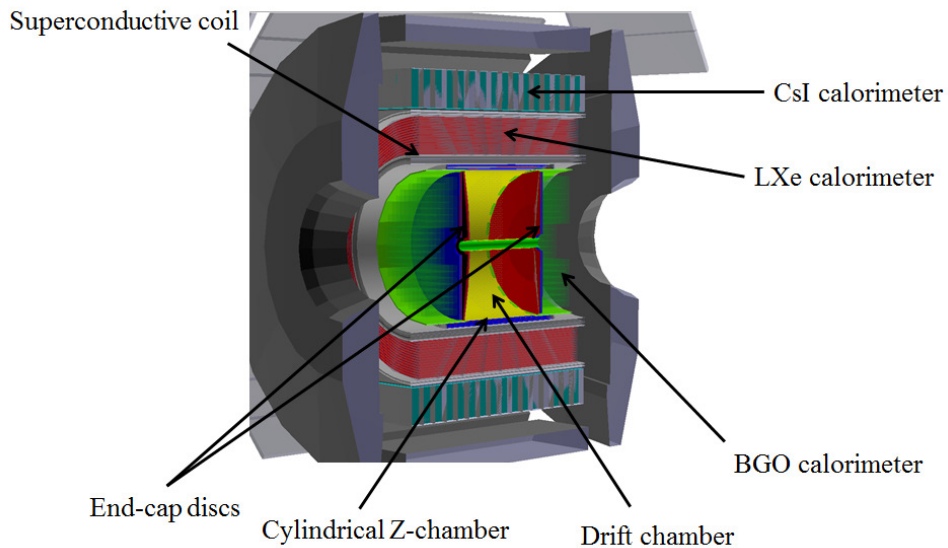
Fig. 5: Spatial resolution of GEM detector at the DEUTERON facility as a function of track angle, determined with 1 GeV electrons [25, 26]. Data are corrected for multiple scattering and the limited resolution of the tracking detectors (details in the text). Only statistical uncertainties are shown.

of the tracking detectors were corrected. The contribution of the multiple scattering to the determined spatial resolution was calculated, based on the value of material budget of the studied detector and the distances between the detectors. This contribution was then quadratically subtracted from the resolution and extracted from the primary co-ordinate residual distributions. The resulting value was divided by $\sqrt{3/2}$ to correct the value of the determined spatial resolution for the limited spatial resolution of the detectors in the experiment. The value $\sqrt{3/2}$ has a statistical origin and is based on the assumption that the tracking detectors in the experiment have the same spatial resolution. The measured spatial resolution of the studied GEM-based detectors for the DEUTERON PTS was extracted as (45 ± 3) μm for electron tracks hitting the detector orthogonally.
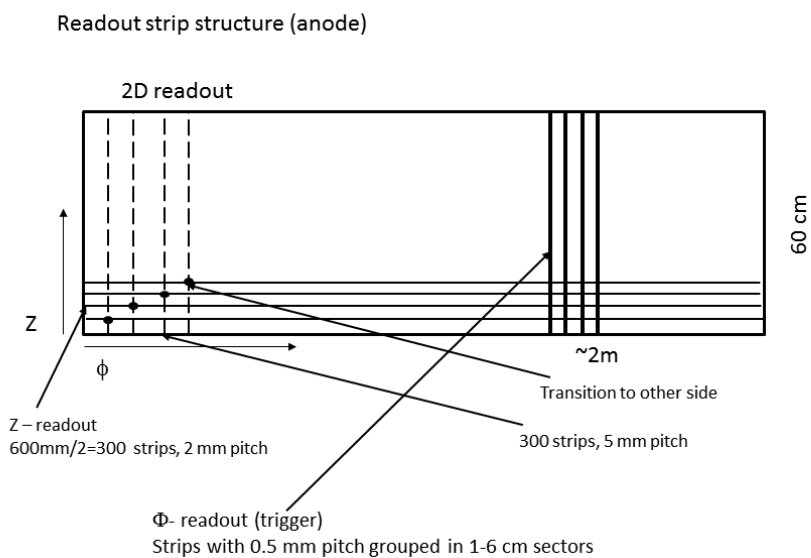
4 Large cylindrical triple-GEM for the CMD-3 detector at the VEPP-2000 collider

Large cylindrical triple-GEM detectors (CGEMs) and flat triple-GEM endcap discs are proposed for the upgrade of the CMD-3 detector at the VEPP-2000 electron–positron collider. The CMD-3 is a general-purpose detector intended for studies of light vector mesons in the energy range between 0.3 GeV and 2.0 GeV [15]. Its structure is shown schematically in Fig. 6. The Z-chamber (ZC) has operated for about 10 years at the VEPP-2M collider [27] and 4 years at the VEPP-2000. Its main purpose is to measure the track co-ordinates precisely along the beam axis (Z co-ordinate) and provide a trigger signal. Some of the ZC parameters have degraded with time. The high-voltage plateau width was reduced from a starting value of 250 V to 50 V, resulting in a decreased efficiency. Therefore, it is necessary to build a new chamber with improved parameters. The CGEM was chosen as utilizing the best technique for this purpose. The inner tracker of the KLOE-II experiment [28], with similar geometrical dimensions, has been constructed, representing a good showcase for the ZC upgrade.
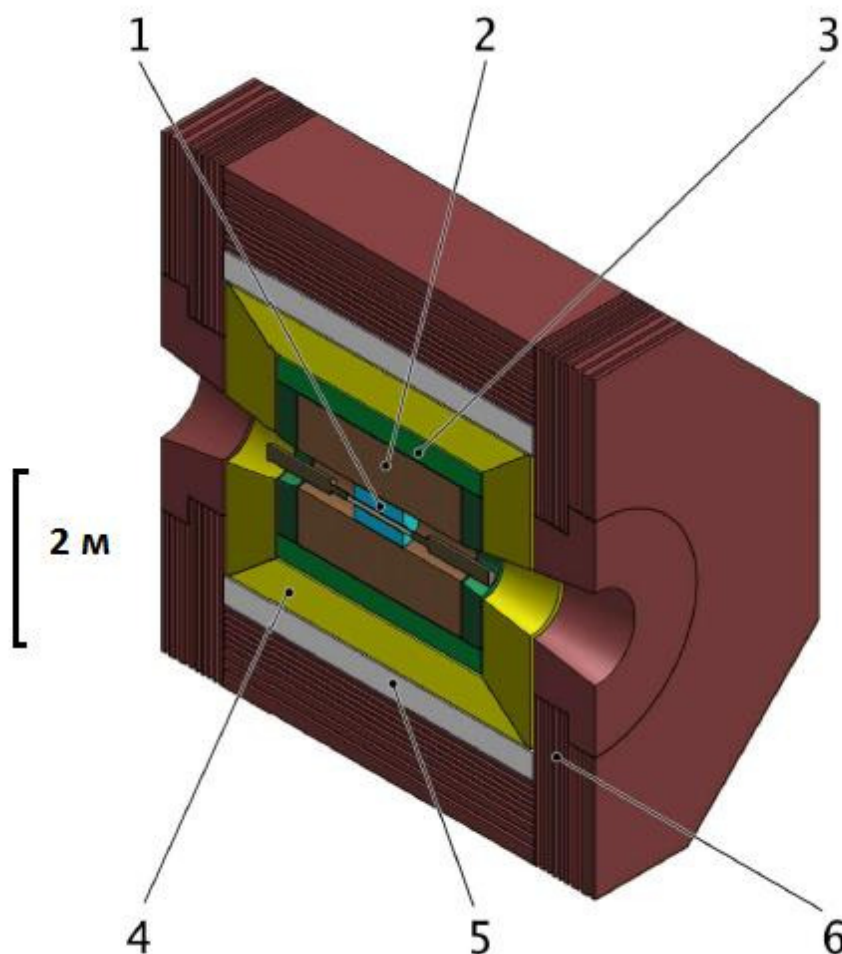
The CGEM is planned to be constructed with a digital readout. The front-end electronics will be situated at the ends of the chamber. A fine segmentation of the anode readout structure can be implemented with modern electronics, using multiplexing (Fig. 7). The double layer of the chamber with a common cathode will allow for a reduction of the systematic errors in the Z co-ordinate determination, owing to the magnetic field and the polar angle of the tracks. One of the most important advantages of the CGEM is the absence of wires, which excludes possible mechanical damage of the wires, such as

Superconductive coil

CsI calorimeter

LXe calorimeter

BGO calorimeter

End-cap discs

Cylindrical Z-chamber

Drift chamber

Fig. 6: CMD-3 detector with all subsystems indicated

Readout strip structure (anode)

2D readout

60 cm

Z

φ

~2m

Transition to other side

Z – readout
600mm/2=300 strips, 2 mm pitch

300 strips, 5 mm pitch

Φ- readout (trigger)
Strips with 0.5 mm pitch grouped in 1-6 cm sectors

Fig. 7: Structure of readout board of CGEM Z-chamber

Fig. 8: General-purpose magnetic detector for Super c-τ Factory with general subsystems indicated. 1: vertex detector; 2: drift chamber; 3: identification system based on FARICH; 4: calorimeter; 5: superconducting coil; 6: yoke with muon system.

breakage or sagging. Another advantage is that the GEM structure has a counting rate capability more than two orders of magnitude higher than the wire chambers. The GEM segmentation allows a part of the chamber to be disconnected in case of damage and high-voltage short circuits after a breakdown; this is impossible with the current ZC. An advantage of the CGEM is the smaller dependence of the effective gain of the GEM cascade on the geometrical accuracy of the chamber than is achieved for the MWPC.

The chamber consists of two concentric triple-GEM detectors with common drift cathode and strip readout boards on the inner and outer cylinders. The chamber diameter and length are both about 60 cm. These dimensions allow one to fabricate each GEM from one piece, approximately 60 cm $\times$ 200 cm rather than gluing several GEM pieces together, as used to be done in the case of the KHLOE-II Inner Tracker [28].

Both the inner and outer readout boards have the same structure as shown schematically in Fig. 7. The PCB has two layers with perpendicular strips, as in the triple-GEM detectors of the COMPASS experiment at CERN [29]. The bottom layer is segmented into 1.9 mm wide strips with a pitch of 2 mm, which provide a measurement of the Z co-ordinate. Each strip is connected through a metallized hole to the opposite side of the PCB, where strips in the perpendicular direction provide signal outputs to the cylinder end. The top layer of the readout board provides trigger signals. It is segmented in strips parallel

to the cylinder axis (Z direction) that are 100–150 µm wide and have a pitch of 500 µm. The trigger strips are connected to each other in groups of 1 cm to 6 cm in size, which will be divided into two halves by the plane at $Z = 0$ mm. The total number of channels used to measure the Z co-ordinate is 300, while the maximum number of trigger channels is 400. The effective pitch of the electronics channels at the cylinder ends will be about 4 mm in this case.

To increase the solid angle coverage of the CMD-3 tracker we propose to set a two-co-ordinate thin (approximately 15 mm) triple-GEM disc detector between the BGO calorimeter and the drift chamber flanges. In this case, the tracker will cover polar angles down to 0.1 rad.

The endcap tracker will provide measurements of the charge asymmetry for the $e^+e^- \to \mu^+\mu^-$ process, which has maximal cross-section at small angles. The high luminosity of the VEPP-2000 and the endcap tracker will enable measurement of the pion form factor over a wide energy range using initial state radiation—a new technique developed at BINP. These disc triple-GEM detectors will look like the detectors built for the TOTEM experiment at CERN [30].

5 GEMs at a vertex detector of the Super c–τ Factory

The conceptual project of the Super c–τ Factory [16] was accepted by BINP in 2013. A study of rare D-mesons and τ-lepton decays, as well as $D^0\overline{D^0}$ oscillations, is the main aim of the Super c–τ Factory physics programme. Another important aim is the search for lepton-flavor-violating decays of the τ-lepton, particularly the $\tau \to \mu\gamma$ decay, which has not yet been observed. The Super c–τ Factory is expected to have a peak luminosity of 10^{35} cm^{-2} s^{-1} in the energy region from 2 GeV to 5 GeV in the centre-of-mass energy frame. A universal collider detector with a magnetic field of approximately 1 T will be mounted in the interaction point of the electrons and positrons. The detector comprises standard subsystems, including a vacuum chamber, a vertex detector, a drift chamber, a particle identification system, an electromagnetic calorimeter, a superconducting coil, and an iron yoke with a muon system (Fig. 8).

Here, the TPC based on GEM detectors is proposed as a vertex detector. The reason for using the GEM detectors for the TPC of the vertex detector is the high rate capability and the possibility of operation in continuous mode, which is not possible for TPCs based on MWPCs. A modern example of the GEM is the development, by ILC Collaboration [31], of a TPC with a continuous readout with GEMs. Also, the ALICE TPC upgrade will utilize GEMs [32]. The continuous readout mode is achieved by a reduction of the ion backflow by more than three orders of magnitude. The first prototypes were tested with a gas mixture of Ar (95%), CF_4 (3%), and C_4H_{10} (2%) in a 5 T magnetic field, parallel to electric field lines up to 15 cm from the readout plane. The spatial resolution in the tests was determined to be approximately 50 µm, with sensitive pads with a surface of 2 mm × 6 mm. It is worth noting that TPCs can implement particle identification based on energy measurements in gas, with dE/dx resolution of a few per cent [31].

6 Conclusions

Tracking detectors based on triple-GEM cascades are being developed and applied in a number of experiments at BINP. GEM detectors have operated at the TS of the KEDR experiment since 2010. The efficiency of these detectors is between 95% and 98% at a gain of 20 000–40 000. The spatial resolution is equal to (65 ± 3) µm for orthogonal electron tracks. The PTS of the DEUTERON facility includes three tracking GEM-based detectors. The detectors are characterized by a low material budget corresponding to $X/X_0 = (2.4 \pm 0.5) \times 10^{-3}$. The spatial resolution of the detectors measured with a 1 GeV electron beam is (45 ± 3) µm for orthogonal tracks.

Large cylindrical triple-GEM detectors and flat triple-GEM endcap discs are proposed for the upgrade of the CMD-3 detector at the VEPP-2000 electron–positron collider. For the upgrade application, the tracker will cover down to polar angles of 0.1 rad, and it will improve the sensitivity of the detector to

processes with small characteristic angles. It is proposed that the vertex detector of the general-purpose magnetic detector for the future Super c–τ Factory at BINP be based on a TPC with GEM detector readout. The experience of the International Linear Collider Collaboration gives reasons to expect that a vertex detector spatial resolution of 50 μm can be achieved.

Acknowledgement

References

[1] F. Sauli, *Nucl. Instrum. Methods Phys. Res. A* **386** (1997) 531, http://dx.doi.org/10.1016/S0168-9002(96)01172-2

[2] B. Ketzer *et al.*, *IEEE Trans. Nucl. Sci.* **49** (2002) 2403, http://dx.doi.org/10.1109/TNS.2002.803891

[3] A. Bressan *et al.*, *Nucl. Instrum. Methods Phys. Res. A* **425** (1999) 262, http://dx.doi.org/10.1016/S0168-9002(98)01406-5

[4] L.I. Shekhtman *et al.*, *J. Instrum.* **7** (2012) C03021, http://dx.doi.org/10.1088/1748-0221/7/03/C03021

[5] L.I. Shekhtman *et al.*, *J. Instrum.* **8** (2013) C12035, http://dx.doi.org/10.1088/1748-0221/8/12/C12035

[6] V.M. Aulchenko *et al.*, *J. Instrum.* **6** (2011) P07001, http://dx.doi.org/10.1088/1748-0221/6/07/P07001

[7] V.V. Anashin *et al.*, *Nucl. Instrum. Methods Phys. Res. A* **478** (2002) 420, http://dx.doi.org/10.1016/S0168-9002(01)01789-2

[8] V.M. Aulchenko *et al.*, *Nucl. Instrum. Methods Phys. Res. A* **355** (1995) 261, http://dx.doi.org/10.1016/0168-9002(94)01093-5

[9] V.V. Anashin *et al.*, *Phys. Part. Nucl.* **44** (2013) 657, http://dx.doi.org/10.1134/S1063779613040035

[10] V.V. Anashin *et al.*, VEPP-4M collider: status and plans, Proc. EPAC'98, Stockholm, 1998, p. 400.

[11] V. Smaluk *et al.* (VEPP-4 Team), Accelerator physics issues of the VEPP-4M at low energy, Proc. of EPAC 2004, Luzern, 2004, p. 749.

[12] S.G. Popov, *Phys. At. Nucl.* **62** (1999) 256.

[13] D.M. Nikolenko *et al.*, *Phys. At. Nucl.* **73** (2010) 1322, http://dx.doi.org/10.1134/S1063778810080065

[14] M.V. Dyug *et al.*, *Nucl. Instrum. Methods Phys. Res. A* **536** (2005) 338, http://dx.doi.org/10.1016/j.nima.2004.08.096

[15] B.I. Khazin *et al.*, *Nucl. Phys. B (Proc. Suppl.)* **181–182** (2008) 376, http://dx.doi.org/10.1016/j.nuclphysbps.2008.09.068

[16] `http://ctd.inp.nsk.su/c-tau/Project/CDR_en_ScTau.pdf`, September 9th 2016.

[17] P. Rossi *et al.*, *Phys. Rev. Lett.* **94** (2005) 012301, http://dx.doi.org/10.1103/PhysRevLett.94.012301

[18] I.A. Koop *et al.*, *Nucl. Phys. B (Proc. Suppl.)* **181–182** (2008) 371, http://dx.doi.org/10.1016/j.nuclphysbps.2008.09.067

[19] D. Berkaev *et al.*, *Nucl. Phys. B (Proc. Suppl.)* **225–227** (2012) 303, http://dx.doi.org/10.1016/j.nuclphysbps.2012.02.063

[20] E.B. Levichev *et al.*, *Phys. Part. Nucl. Lett.* **13** (2016) 7, http://dx.doi.org/10.1134/S154747711607044X

[21] V.M. Aulchenko *et al.*, *Nucl. Instrum. Methods Phys. Res. A* **494** (2002) 241, http://dx.doi.org/10.1016/S0168-9002(02)01474-2

[22] V.M. Aulchenko *et al.*, *Nucl. Instrum. Methods Phys. Res. A* **598** (2009) 112, http://dx.doi.org/10.1016/j.nima.2008.08.115

[23] M.V. Dyug *et al.*, *Nucl. Instrum. Methods Phys. Res. A* **495** (2002) 8, http://dx.doi.org/10.1016/S0168-9002(02)01572-3

[24] A. Bondar *et al.*, *Nucl. Instrum. Methods Phys. Res. A* **556** (2006) 495, http://dx.doi.org/10.1016/j.nima.2005.11.098

[25] V.S. Bobrovnikov *et al.*, *J. Instrum.* **9** (2014) C08022, http://dx.doi.org/10.1088/1748-0221/9/08/C08022

[26] G.N. Abramov *et al.*, *J. Instrum.* **11** (2016) P03004, http://dx.doi.org/10.1088/1748-0221/11/03/P03004

[27] E.V. Anashkin *et al.*, *Instrum. Exp. Tech.* **6** (2006) 798, http://dx.doi.org/10.1134/S0020441206060066

[28] A. Balla *et al.*, *Nucl. Instrum. Methods Phys. Res. A* **628** (2011) 194, http://dx.doi.org/10.1016/j.nima.2010.06.315

[29] B. Ketzer *et al.*, *IEEE Trans. Nucl. Sci.* **48** (2001) 1065, http://dx.doi.org/10.1109/23.958724

[30] G. Antchev *et al.*, *Nucl. Instrum. Methods Phys. Res. A* **617** (2010) 62, http://dx.doi.org/10.1016/j.nima.2009.08.083

[31] M. Dixit *et al.*, *Nucl. Instrum. Methods Phys. Res. A* **581** (2007) 254, http://dx.doi.org/10.1016/j.nima.2007.07.099

[32] ALICE Collaboration. Technical design report for the upgrade of the ALICE time projection chamber. ALICE-TDR-016, CERN-LHCC-2013-020, (CERN, Geneva, 2013), `http://cds.cern.ch/record/1622286/files/ALICE-TDR-016.pdf`